Formation and Properties of Polystyrene-*block*-poly(2-hydroxyethyl methacrylate) Micelles

Guojun Liu,* Carl K. Smith,† Nanxing Hu, and Jian Tao

Department of Chemistry, University of Calgary, 2500 University Drive, NW, Calgary, Alberta, Canada T2N 1N4

Received March 21, 1995; Revised Manuscript Received October 11, 1995[⊗]

ABSTRACT: Polystyrene-*block*-poly(2-hydroxyethyl methacrylate) (PS-*b*-PHEMA) samples of different molar masses have been synthesized. These polymers formed micelles in THF/cyclohexane mixtures. The change in the hydrodynamic radius and aggregation number of these micelles as a function of cyclohexane volume fraction f_c has been investigated. We also report some preliminary fluorescence results of pyrene- and fluorene-labeled PS-*b*-PHEMA. The increase in energy transfer from fluorene, attached randomly at a density of <5% to the PHEMA block, to pyrene, attached at the junction point between PS and PHEMA, provides a sensitive measure for micelle formation. The energy transfer efficiency in micelles was high, and excimer formation between different fluorene groups was negligible. This will facilitate micellar core size determination by energy migration.

I. Introduction

Due to their potential medical and pharmaceutical applications, diblock copolymer micelles have attracted much attention in the past decade.[1−4] Much insight has been gained into the understanding of the equilibrium properties[5−19] and the chain exchange dynamics[20−24] of diblock copolymer micelles.

Of all the techniques used for diblock micelle studies, fluorescence spectroscopy has gained popularity only recently. It has now been used for probing the onset of micellization,[13−16] the relaxation kinetics,[24−26] and the local viscosity, polarity, and structure of micelles[27−29] as well as for following the uptake of hydrophobic moieties by micellar cores from an aqueous medium.[18,28] Fluorescence techniques can also be used for the determination of the core size[30] and the rate constant of chain exchange[31] of micelles as expounded recently by one of us.

It is for the ultimate objective of carrying out chain exchange kinetic studies that we have synthesized the following polystyrene (PS) and poly(2-hydroxyethyl methacrylate) (PHEMA) block copolymers:

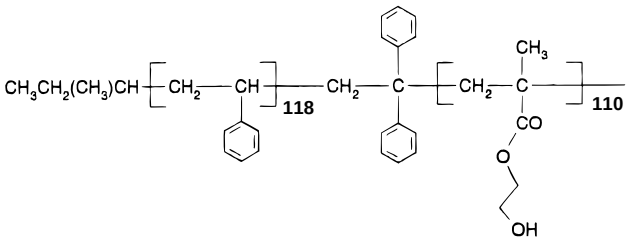

Ia

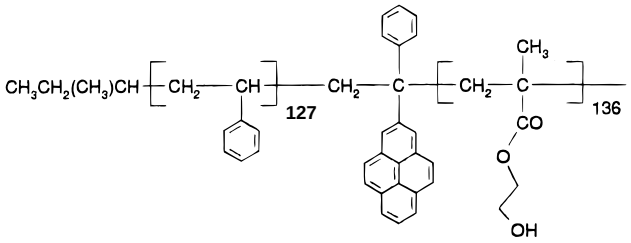

Ib

To perform such an experiment,[31] the PHEMA blocks of polymers Ia and Ib will be labeled with less than 5% fluorene. A micelle solution of polymer Ia-Fl(*y*), polymer Ia labeled with fluorene at a density *y*, will be first prepared in which the core would consist of the labeled PHEMA block. After the mixing of a polymer Ia-Fl(*y*) micelle solution with a polymer Ib-Fl(*y*) unimer solution, either the decrease in the fluorescence intensity of the fluorene group, the donor, or the increase in that of the pyrene group, the acceptor, as a function of time will be monitored and the data will then be analyzed to generate the rate constant for unimer incorporation into micelles.

The present study has been meant to pave the way for our future determination of the core size and the chain exchange rate constant of PS-*b*-PHEMA micelles by establishing the conditions for micelle preparation from these polymers. To see how the length of the diblock copolymer affects micellar properties, polymer II has been synthesized:

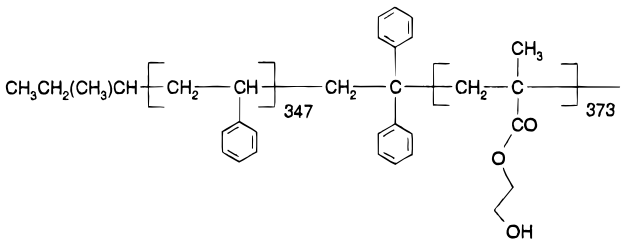

II

In section II, we describe the experimental details. How the hydrodynamic radius R_H, intrinsic viscosity $[\eta]$, and aggregation number *p* of polymer Ia and II micelles in THF/cyclohexane change as a function of cyclohexane content will be reported in section III. We also show some preliminary fluorescence results obtained using polymer Ia-Fl(*y*) and polymer Ib-Fl(*y*). Some conclusions are reached in section IV.

II. Experimental Section

Polymer Synthesis. Solvent THF was dried by refluxing in the presence of potassium under argon. Styrene was first filtered through an alumina column and then stirred with benzylmagnesium chloride at room temperature for 3 h. The monomer was freshly distilled under reduced pressure for each

* To whom correspondence should be addressed.
† Now at Schlumberger Cambridge, High Cross, Madingley Road, Cambridge, U.K. CB3 OEL.
⊗ Abstract published in *Advance ACS Abstracts,* December 1, 1995.

0024-9297/96/2229-0220$12.00/0

Scheme 1

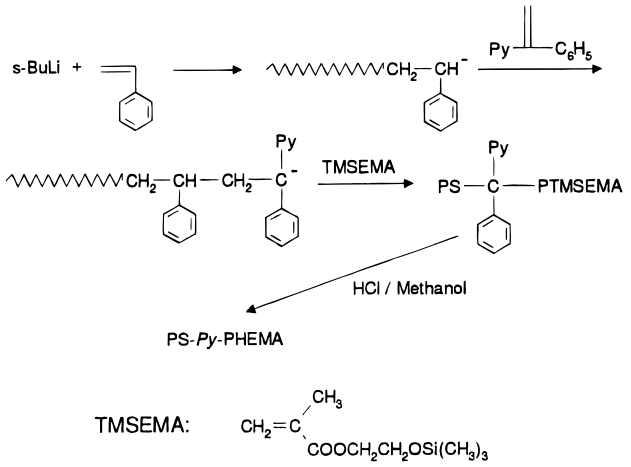

polymerization. Monomer 2-[(trimethylsilyl)oxy]ethyl methacrylate was synthesized following a literature method[32] and was purified by distilling from CaH_2 and then from triethylaluminum under reduced pressure. 1-(1′-Pyrenyl)-1-phenylethylene (PyPE) was also prepared following a literature method[33] and purified by recrystallization twice from diethyl ether. 1,1-Diphenylethylene (Aldrich, 97%) was vacuum distilled over *n*-butyllithium before use.

Polymer Ib was synthesized following Scheme 1.[34] Styrene was first polymerized at −78 °C in THF using *sec*-butyllithium. After 30 min, an aliquot of the polymerization mixture was taken and the PS homopolymer was precipitated out from methanol for GPC analysis. To the remaining reaction mixture were then added PyPE and lithium chloride, each at a concentration 3 times that of the initiator. PyPE reacted with polystyryl anions to produce the sterically more hindered PS−PyPE anions. Lithium chloride was used to reduce the molar mass distribution of the second block. After 30 min of stirring, (trimethylsiloxy)ethyl methacrylate (TMSEMA) was added dropwise over a time span of 20 min. The polymerization of TMSEMA was allowed to proceed for another 0.5 h before being terminated by the addition of ∼2.0 mL of methanol. The mixture was then allowed to warm to room temperature, and 2 mL of methanol and 2 mL of 10% hydrochloric acid were added to catalyze the hydrolysis of the trimethylsilyl group of the PTMSEMA block for 30 min. The polymer solution was then poured into water to precipitate out the polymer. The solid precipitate was filtered, dried, and extracted in refluxing cyclohexane for 3−4 h to remove the PS homopolymer. PS-*Py*-PHEMA was further purified by dissolving in THF and precipitation into an ether/pentane mixture at a 1:1 volume ratio.

Polymers Ia and II were synthesized in a similar fashion except that the use of PyPE was replaced by 1,1-diphenylethylene.

Polymer Characterization. GPC analysis of the PS blocks and all diblocks was done using a Varian Model 5000 HPLC instrument and a Styragel HR 4 (Waters) column calibrated using monodisperse polystyrene standards (Polymer Laboratories) in THF. Before GPC analysis, the PHEMA block of each sample was esterified by cinnamoyl chloride in pyridine.

Esterified diblocks dissolved in $CDCl_3$ were also analyzed using ^{1}H NMR to obtain the ratio of the number of styrene units to that of the HEMA units, n/m. The absolute weight-average molar masses of diblocks were determined using a Brookhaven Model 9025 light scattering instrument equipped with a 10-mW helium−neon laser at scattering angles between 25 and 140° in toluene. Samples used for light scattering measurement were subjected to filtration through GPC columns to remove impurity particles. The difference Δn_r in the refractive index of a polymer solution and that of pure toluene at 633 nm was determined using a differential refractometer (Precision Instruments Co.) equipped with a band-pass filter at room temperature.

Fluorene Labeling of PHEMA. Fluorene labeling of the PHEMA block of polymers Ia and Ib was achieved by reacting these polymers with a controlled amount of 9-fluoreneacetic anhydride in dry pyridine under an argon atmosphere at room temperature for 24 h. 9-Fluoreneacetic anhydride was prepared by reacting 2 molar equiv of 9-fluoreneacetic acid (Aldrich) with 1.2 equiv of thionyl chloride in dry pyridine.[35] The resultant product was purified by recrystallizing from hexane.

Preparation of Micelle Solutions. A polymer was fully dissolved in distilled THF in an ampule first. A designated amount of cyclohexane was then added to the THF solution to make up a certain THF/cyclohexane volume ratio. The mixture was then sealed in the ampule using a torch and heated at ∼50 °C for 3−4 h before any physical measurements were carried out.

Dynamic Light Scattering. The hydrodynamic radii R_H of micelles were determined at room temperature, i.e., 22 ± 0.5 °C, by photon correlation spectroscopy using a Brookhaven BI2030 instrument with 280 channels. A Lexel 2-W argon ion laser, with emission at $\lambda = 514.5$ nm, was used as the light source. The typical micelle concentration used was ∼1 mg/mL, and the scattering angle θ was 135°. The autocorrelation function G_{vv} of the scattered polarized light was analyzed using the standard cumulant fit software provided by Brookhaven Instruments to obtain the mean decay rate Dq^2 for each sample, where D is the mean diffusion coefficient of micelles and q is the scattering vector with its magnitude given by

$$q = \frac{4\pi n_r}{\lambda} \sin(\theta/2) \tag{1}$$

In eq 1, λ is the wavelength of the laser beam; n_r, the refractive index of the binary solvent mixture used, is calculated from the refractive indices n_1 and n_2 of the individual solvents using[36]

$$(1/\rho)(n_r - 1) = (w_1/\rho_1)(n_1 - 1) + (w_2/\rho_2)(n_2 - 1) \tag{2}$$

where w_1 and w_2 are the weight fractions of components 1 and 2, respectively, and ρ_1 and ρ_2 are their densities. In our case, n_1 and n_2 for THF and cyclohexane at 514.5 nm have been approximated by 1.4050 and 1.4266, the refractive indices of THF and cyclohexane at the sodium line.[37]

The mean hydrodynamic radius R_H was then calculated from D using the Stokes−Einstein relation:

$$D = \frac{kT}{6\pi\eta_0 R_H} \tag{3}$$

where kT refers to the thermal energy at temperature T and η_0 the zero-shear-rate viscosity of a THF/cyclohexane mixture, which we determined experimentally.

For viewing the distribution in R_H, the autocorrelation function G_{vv} of scattered light intensities was analyzed using an exponential sampling program called CONTIN.

Viscosity Measurement. The viscosities of solvents and polymer micelle solutions were measured using a Cannon Ubbelohde type viscometer immersed in a water bath equilibrated at either 25.0 or 22.0 °C. Since the flow times were all above 100 s, no kinetic energy corrections were made in calculating the viscosity from the flow time values. The viscosity η_0 of a THF/cyclohexane mixture was, for example, calculated by ratioing the flow time t_0 of the mixture to that t_w of water using

$$\eta_0 = (t_0\rho_0/\rho_w t_w)\eta_w \tag{4}$$

where ρ_0 and ρ_w are the densities of the solvent mixture and water, respectively; η_w, the viscosity of water, is 0.961 cP at 21.8 °C.[37]

The intrinsic viscosity $[\eta]$ of micelles in a given solvent mixture is obtained by plotting reduced viscosity η_{red} versus polymer concentration c and extrapolating to zero concentration. The reduced viscosity of a micelle solution is calculable

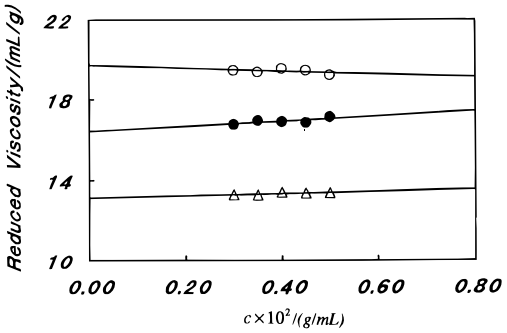

Figure 1. Reduced viscosities of polymer II as a function of concentration at the solvent compositions of $f_c = 0.20$ (○), $f_c = 0.40$ (●), and $f_c = 0.70$ (△), respectively.

from micelle solution flow time t_m and solvent flow time t_0 using

$$\eta_{red} = \frac{t_m - t_0}{t_0 c} \quad (5)$$

Illustrated in Figure 1 is a plot of η_{red} versus c for polymer II micelles at the cyclohexane volume fraction f_c of 20, 40, and 70%, respectively. The corresponding intrinsic viscosities are 19.7, 16.4, and 13.1 cm^3/g.

UV Measurement. All UV spectra and absorbance values were obtained on a Perkin-Elmer 3480 photodiode spectrophotometer.

Fluorescence Measurements. Steady-state fluorescence measurements were carried out on a Photon Technologies International (PTI) Alphascan instrument with a 75-W Xe lamp as the excitation source. Emission spectra were not corrected for the wavelength-dependent response of the emission monochromator and the photomultiplier tube. Narrow slit widths, e.g. <2.0 nm, were used for most studies. The typical polymer concentration used was 0.20 mg/mL.

Fluorescence lifetimes were measured using an LS100 time-correlated single-photon-counting apparatus (PTI). A thyratron-gated hydrogen discharge lamp was used as the excitation source.

III. Results and Discussion

NMR Characterization of the Polymer Samples. Three samples were used in this study. Polymers Ia and Ib were synthesized supposedly with 100 repeat units of styrene and HEMA. Illustrated in Figure 2 is a ^{1}H NMR spectrum of polymer Ia esterified with cinnamoyl chloride, i.e., polystyrene-*b*-poly(cinnamoylethyl methacrylate) or PS-*b*-PCEMA. From ratioing the proton peak intensity of PCEMA at δ 7.66 (d, 1H, 15.9 Hz) or 4.17 (d, 4H, 24.5 Hz) to that of PS at δ 7.15 (b, 3H), we obtained a styrene to CEMA ratio, i.e., n/m, of 1.07, which is, within experimental error, the same as 1.00. Similarly, we determined the n/m ratios for polymers Ib and II to be 0.93.

Our NMR results clearly indicated that the conversion of PHEMA to PCEMA approached 100%. This high conversion may have arisen from the accessibility of hydroxyl groups of PHEMA, as they are relatively far from the backbone.

GPC Characterization of the Polymer Samples. Since the GPC columns were calibrated using PS standards, the molar masses determined for diblocks were not meaningful. We have thus only retained the characterization results of the PS block of each polymer in Table 1. Also retained are the polydispersity indices of the diblocks. These values suggest that both the PS blocks and our diblocks have narrow molar mass distributions.

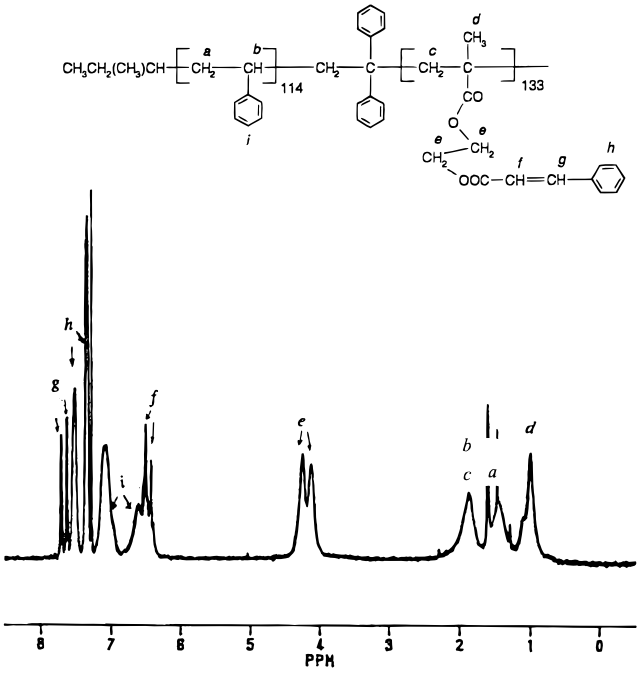

Figure 2. ^{1}H NMR spectrum of polymer Ia esterified by cinnamic acid chloride.

Table 1. Summary of Characterization Results for the Polymers

	PS block (GPC)			block copolymer			
polymer	$\bar{M}_w$ (g/mol)	$\bar{M}_n$ (g/mol)	$\bar{M}_w/\bar{M}_n$	$\bar{M}_w/\bar{M}_n$ GPC[a]	$\bar{M}_w$ (g/mol) LS[a]	n/m NMR	$\bar{n}_w$[b] LS and NMR
Ia	0.90×10^4	0.84×10^4	1.08	1.09	4.1×10^4	1.07	118
Ib	0.97×10^4	0.90×10^4	1.08	1.17		0.93	127[c]
II	3.5×10^4	3.1×10^4	1.13	1.09	13.3×10^4	0.93	347

[a] PS-*b*-PHEMA was esterified using cinnamoyl chloride and then analyzed. [b] These represent the weight-average numbers of repeat units for PS. [c] Estimated based on the $\bar{n}_w$ value of polymer Ia and the comparison of the GPC data of polymers Ia and Ib.

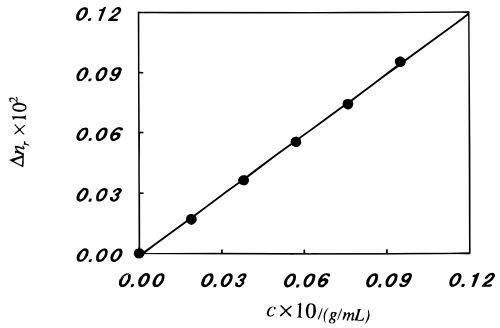

Figure 3. Differences Δn_r between the refractive indices of polymer II solutions and toluene as a function of polymer II concentration c.

Specific Refractive Index Increment ν of the Polymer Samples. Figure 3 illustrates how the difference Δn_r between the refractive index of a polymer Ia solution and that of pure toluene varies with polymer concentration c. The best fit to the data using

$$\Delta n_r = a_0 + \nu c \quad (6)$$

yielded the specific refractive index increment value ν or dn_r/dc value of 0.100 mL/g as shown in Table 2. In a similar fashion, we have obtained the ν values of 0.101, 0.112, and 0.094 mL/g for polymer II, a PS standard (Polysciences: $\bar{M}_w = 3.0 \times 10^4$ g/mol), and a PCEMA sample synthesized by us, respectively.

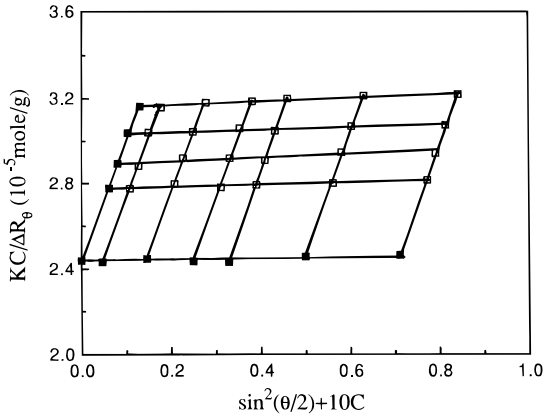

Figure 4. Light scattering data of polymer Ia plotted as a function of $\sin^2(\theta/2) + 10c$.

Table 2. Characterization of Cinnamoyl Chloride Esterified Polymers by Light Scattering

polymer	dn/dc (mL/g)	$\bar{M}_w$* (g/mol)	$\bar{M}_w$ (g/mol)
Ia	0.100	4.1×10^4	4.1×10^4
II	0.101	12.8×10^4	13.3×10^4

Polymer Characterization by Static Light Scattering. In Figure 4, light scattering data of polymer Ia in toluene have been plotted versus $\sin^2(\theta/2) + 10c$. Extrapolating the data to zero c and zero θ yielded the apparent molar mass $\bar{M}_w$* of 4.1×10^4 g/mol for polymer Ia, as tabulated in Table 2. Since the specific refractive index increments of the two blocks relative to toluene are different, the apparent molar mass should be corrected to obtain the true molar mass $\bar{M}_w$. $\bar{M}_w$* is related to $\bar{M}_w$ of polymer II by[36]

$$\bar{M}_w^*/\bar{M}_w = \frac{1}{\nu^2}[\nu_1\nu_2 - (\nu_1\nu_2 - \nu_2^2)w_{PS}^2 - (\nu_1\nu_2 - \nu_1^2)(1 - w_{PS})^2] \quad (7)$$

where ν_1 and ν_2, 0.938 and 0.112 mL/g, are the specific refractive index increments of PCEMA and PS, respectively, and ν is that of polymer Ia. Using the above equation, we have calculated $\bar{M}_w$ for polymer Ia to be 4.1×10^4 g/mol, as shown in Table 2. Similarly, we determined the $\bar{M}_w$ of 13.3×10^4 g/mol for polymer II.

Summary of Polymer Characterization Results. Using the PS repeat unit molar mass of 104 g/mol and $\bar{M}_w = 3.5 \times 10^4$ g/mol for the PS block of polymer II from GPC, we obtained the weight-average number of repeat units, $\bar{n}_w$, of 337 for PS. Based on $\bar{M}_w = 13.3 \times 10^4$ g/mol, from light scattering, of the cinnamoyl-esterified polymer II and the n/m ratio of 0.93 determined by NMR, we calculated an $\bar{n}_w$ value of 347, which is in good agreement with 337 from GPC. Similarly, we found $\bar{n}_w = 87$ from GPC and $\bar{n}_w = 118$ from light scattering and NMR measurement for polymer Ia. The reason for the relatively large discrepancy between $\bar{n}_w$ from different approaches for polymer Ia is unknown.

We did not carry out light scattering studies of polymer Ib. From ratioing the GPC $\bar{M}_w$ data of the PS blocks of polymers Ia and Ib, we estimated an $\bar{n}_w$ value of 127 for polymer Ib.

UV Characterization. Illustrated in Figure 5 is the comparison between the absorption spectra of polymer Ia-Fl(2.4%), polymer Ib, and polymer Ib-Fl(4.0%) in THF. In the wavelength region from 320 to 360 nm, fluorene absorbs negligibly and pyrene can be excited selectively. Fluorene, on the other hand, can be selectively excited between 290 and 305 nm.

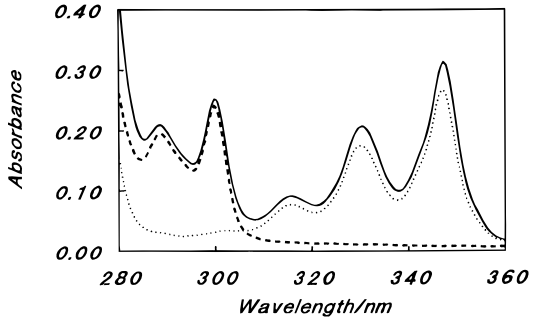

Figure 5. UV−visible absorption spectra of polymer Ib (···), polymer Ia-Fl(2.4%) (- - -), and polymer Ib-Fl(4.0%) (—).

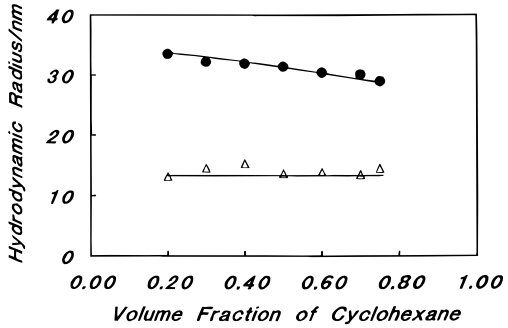

Figure 6. Change in the hydrodynamic radius R_H of polymer Ia (△) and polymer II (●) micelles as a function of cyclohexane volume fraction f_c.

So far, we have not carried out any detailed characterization of polymers Ia and Ib labeled with different amounts of fluorene. Our preliminary analysis, based on the assumption that fluorene and pyrene have extinction coefficients of ~8000 and ~40 000 cm^{-1} M^{-1} at 290 and 348 nm,[38] has indicated that we were able to label the hydroxyl groups of the PHEMA block of polymers Ia and Ib with 9-fluoreneacetic anhydride with an efficiency close to 100%: i.e., 1 mol of 9-fluoreneacetic anhydride reacts with 1 mol of PHEMA hydroxyl groups. The fluorene labeling densities of 2.4 and 4.0% and those quoted later on represent the stoichiometric ratios between 9-fluoreneacetic anhydride and hydroxyl groups used in our labeling experiments.

Dynamic Light Scattering Results. Micelle formation from polymer II, induced by the addition of cyclohexane to a polymer solution in THF, could be seen with the naked eye as such a micelle solution would have a characteristic bluish tinge. The sizes of polymer Ia and Ib micelles are smaller, and the light scattering instrument was required for the unambiguous identification of micelle formation.

For $f_c < 0.20$, micelle formation was not extensive, scattered light intensity was low, and we did not determine the hydrodynamic radius of these samples. For $f_c \geq 0.20$, the change in the mean hydrodynamic radius R_H of polymer II and Ia micelles as a function of solvent composition is illustrated in Figure 6.

For $0.20 \leq f_c \leq 0.75$, the sizes of polymer II micelles are larger than those of polymer Ia, a trend in agreement with the prediction of scaling theories.[3] Scaling theories have been used to derive relations between the length of a diblock copolymer and the size of "hairy" and "crew-cut" micelles. In a hairy micelle, the core block is much shorter than the corona block and the radius R

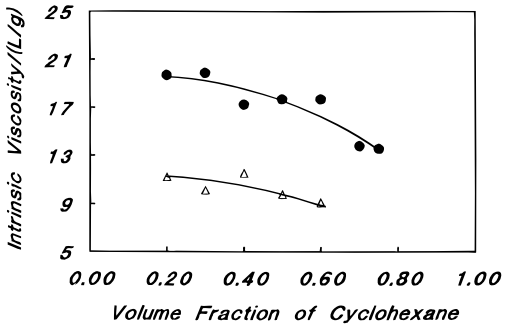

Figure 7. Change in the intrinsic viscosity of polymer Ia (△) and polymer II (●) micelles as a function of f_c.

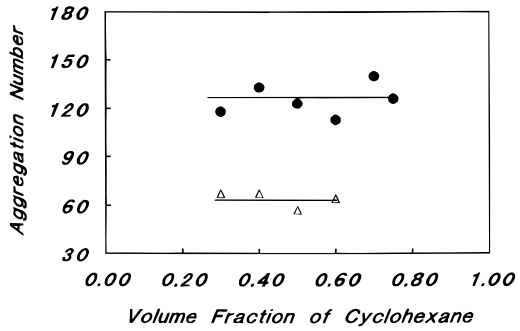

Figure 8. Change in the aggregation number of polymer Ia (△) and polymer II (●) micelles as a function of f_c.

of a micelle is chiefly determined by the thickness of the corona, which scales as

$$R \propto m^{4/25} n^{3/5} \tag{8}$$

where m and n represent the number of units in the core and corona blocks, respectively. In a crew-cut micelle, the radius R, now governed by the core size, scales according to

$$R \propto m^{2/3} \tag{9}$$

With our samples, the lengths of the core and corona blocks are comparable, and no simple scaling relations exist between R and n and m. One would intuitively still expect R to increase with n and m.

As the solvent quality for the PHEMA block worsens, the hydrodynamics radius R_H seems to decrease for polymer II micelles but remains constant for polymer Ia micelles. These results seem to contradict the theoretical prediction of Munch and Gast.[9] Their numerical analysis showed that as the solvent quality for the core block worsened, the corona thickness increased, the core diameter decreased, and the overall radius of the micelle, e.g., R_H, increased. A possible reason for the discrepancy is that our experimental situation is different from what was examined by Munch and Gast. Munch and Gast examined the effect of adding more and more of a solvent which is poor for the core but good for the corona block on the change of micelle sizes. Cyclohexane here at room temperature borders between a Θ and a poor solvent for PS as the Θ temperature is at 34.5 °C.[39] As more and more cyclohexane is added to the polymer solution in THF, a good solvent for PS, the corona layer may not expand as much as it would if cyclohexane was a good solvent. This hypothesis seems to explain the R_H results of polymer Ia micelles as well. The molar mass of the PS block of polymer Ia is only $\sim 1.0 \times 10^4$ g/mol. Cyclohexane may be reasonably good for PS with such a low molar mass. Upon the addition of cyclohexane, the PS block of polymer Ia may expand more significantly than in the polymer II case, which makes R_H of polymer Ia micelles more or less constant at all f_c examined.

Examination of the R_H distribution of polymer Ia and II micelles revealed that polymer II forms more stable micelles. While polymer II micelles had a single-peak R_H distribution at all f_c values examined, polymer I was seen to form a small amount of aggregates with sizes larger than those of micelles at $f_c > 0.60$.

Viscosity Results. The intrinsic viscosities of polymer Ia and II micelles are plotted as a function of f_c in Figure 7. The relatively larger error in the data can be partially attributed to the use of mixed solvents and relatively dilute polymer solutions in our measurements. A micellar solution was prepared by first dissolving a certain amount of polymer in THF. Cyclohexane was then added so that a certain THF/cyclohexane ratio was achieved. As a solvent at this THF/cyclohexane ratio was then prepared separately, any mismatch in solvent composition in the two cases can introduce an error in the flow times and subsequently in the reduced viscosity. The error due to solvent composition mismatch can be largely removed if the polymer solutions are made more concentrated. We could not do that as we had a limited amount of polymer samples.

The intrinsic viscosities of polymer Ia micelles at $f_c = 0.70$ and $f_c = 0.75$ could not be measured. This is due to the fact that polymer Ia micelles with concentrations higher than ~3 mg/mL underwent phase separation at these solvent compositions as was evidenced by the difficulty with filtering these samples through a 0.45-μm Millipore filter. Light scattering and fluorescence studies of these samples were possible as lower polymer concentrations were employed.

The intrinsic viscosities of polymer Ia and II micelles seem to decrease as f_c increases. Since the intrinsic viscosity is given by

$$[\eta] = \frac{10\pi R_H^3}{3M_M} \tag{10}$$

where M_M is the molar mass of the micelle, the decrease in $[\eta]$ with f_c may be due to a decrease in either R_H or the aggregation number p of micelles. In the next section, we will combine R_H determined from light scattering and $[\eta]$ to show that the aggregation number p stays approximately constant at all f_c examined.

Aggregation Number *p*. Rearranging eq 10 and using $M_M = p\bar{M}_w$, we obtain

$$p = \frac{10\pi N_A R_H^3}{3[\eta]\bar{M}_w} \tag{11}$$

where $\bar{M}_w$ is the molar mass of the constituent diblock copolymer of a micelle. Using eq 11, we have calculated the aggregation numbers p of polymer Ia and II micelles at different f_c, and the results are plotted in Figure 8. The fluctuation in p is mainly caused by the scatter in $[\eta]$ data. Within experimental error, p does not vary with the solvent composition.

The p values are ~64 and ~126 for polymer Ia and II micelles, respectively. At an almost constant n/m, that p increases with polymer length is in agreement with the numerical analysis results of Munch and Gast[9] and scaling theories of "crew-cut" and "hairy" micelles.[3]

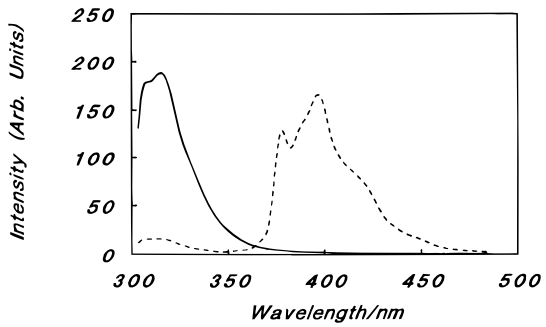

Figure 9. Comparison of the fluorescence spectra of polymers Ia (—) and Ib (- - -) both labeled at a fluorene density of 2.4% in a THF/cyclohexane mixture with $f_c = 0.75$.

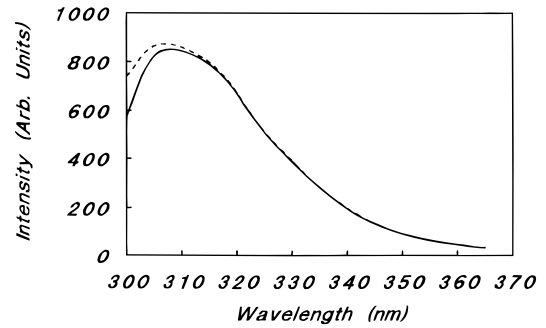

Figure 10. Comparison between the fluorescence spectrum of polymer Ia-Fl(0.3%) (—) and that of polymer Ia-Fl(2.4%) (- - -).

Fluorescence Properties of Labeled Micelles. Illustrated in Figure 9 is the comparison between the fluorescence spectrum of polymer Ia-Fl(2.4%) and that of polymer Ib-Fl(2.4%) in a 75/25 (v/v) cyclohexane/THF mixture. It is obvious that the fluorene emission is well resolved from the pyrene emission centered around 400 nm.

Since similar conditions, i.e., equal fluorene absorbance at 288 nm and equal excitation and emission slit widths, were used for obtaining the spectra in Figure 9, the decrease in the fluorene emission intensity of polymer Ib-Fl(2.4%) relative to that of polymer Ia-Fl(2.4%) suggests significant quenching of fluorene fluorescence by pyrene in the latter system. Fluorene emission intensity ratioing yielded a quenching efficiency χ of 85%.

Fluorene fluorescence may be quenched by fluorene excimers or by pyrene. Illustrated in Figure 10 is the comparison between polymer Ia-Fl(y) at the labeling densities of 0.3 and 2.4%, respectively, at $f_c = 0.60$. Other than the discrepancy between 300 and 308 nm, the emission spectra are the same between 308 and 365 nm for the two samples. The higher intensity of polymer Ia-Fl(0.3%) between 300 and 308 nm derives from its stronger scattering effect, as a higher concentration was required of polymer Ia-Fl(0.3%) to obtain a fluorescence spectrum which was of similar intensity as that of polymer Ia-Fl(2.4%). That the two spectra coincide with one another well between 308 and 365 nm suggests that fluorene excimer formation inside a micelle core is negligible for $y < 2.4\%$. In fact, we have examined samples with $y = 6.0$ and 10.0%, and excimer formation was not observed for these samples either. The low excimer formation of fluorene is partially due to the high viscosity of the micelle cores in which fluorene is. It is also partially due to the fact that excimer formation is not significant for fluorene at room temperature as noted by Horrocks and Brown.[40] The negligible fluorene excimer formation suggests that energy transfer from fluorene to its excimers will not be a dominant quenching mechanism, and this feature will be highly desirable for the core size determination of PS-*Py*-PHEMA-Fl(y) micelles by energy migration.[30]

The absence of fluorene fluorescence quenching by excimers suggests that pyrene will be the main quencher. Pyrene may quench fluorene fluorescence by mechanisms, such as radiationless deactivation, other than energy transfer. We have determined the efficiency of fluorene fluorescence trapping by pyrene, E_T, following a technique developed by Liu and Guillet.[41] If $E_T = \chi$, the quenching of fluorene fluorescence by mechanisms other than energy transfer to pyrene will be ruled out.

Using the Liu and Guillet technique, one measures pyrene fluorescence intensities $I(\lambda_1)$ and $I(\lambda_2)$ when selectively exciting fluorene and pyrene at wavelengths λ_1 and λ_2, respectively. Then one determines the absorbances $A(\lambda_1)$ and $A(\lambda_2)$ of the sample at λ_1 and λ_2 and the ratio of light intensities from the excitation source at these two wavelengths, $I_0(\lambda_2)/I_0(\lambda_1)$, using a Rhodamine B quantum counter. E_T can be calculated using

$$E_T = \frac{1}{P}\left[\frac{I(\lambda_1)I_0(\lambda_2)(1 - 10^{-A(\lambda_2)})}{I(\lambda_2)I_0(\lambda_1)(1 - 10^{-A(\lambda_1)})} - 1 + P\right] \quad (12)$$

where P is the fraction of light absorbed by fluorene out of the total amount of light absorbed at λ_1 and can be evaluated using

$$P = \frac{1 - 10^{-A_F(\lambda_1)}}{2 - 10^{-A_F(\lambda_1)} - 10^{-A_{Py}(\lambda_1)}} \quad (13)$$

In eq 13, $A_F(\lambda_1)$ and $A_{Py}(\lambda_1)$ are absorbances of fluorene and pyrene at λ_1, respectively. $A_{Py}(\lambda_1)$ can be estimated from pyrene absorbance $A(\lambda_2)$ at wavelength λ_2, at which only pyrene absorbs, and the ratio of pyrene absorbances at λ_1 and λ_2 as determined from polymer Ib.

In our measurements, λ_1 and λ_2 were chosen so that $A(\lambda_1)$ and $A(\lambda_2)$ would have similar values. The frequently used λ_1 were 288 (maximum), 295 (minimum), and 298 nm (maximum). Similarly, the λ_2 were chosen to correspond to one of the absorption maxima or minimum in the 320−360 nm range.

We have determined that $E_T = 84\%$ for polymer Ib-Fl(2.4%) in a 75/25 (v/v) cyclohexane/THF mixture. This is, within experimental error, the same as 85%, the quenching efficiency, and suggests that fluorene fluorescence was quenched by pyrene due to energy transfer only. The agreement between the quenching efficiency and energy trapping efficiency also suggests that fluorene fluorescence cannot be quenched by fluorene excimers.

Micelle Formation and Energy Transfer. As f_c increased, E_T increased for polymer Ib-Fl(2.4%) as shown in Figure 11. The abrupt increase in E_T with f_c between 0.10 and 0.20 suggests that micelle formation occurs during that f_c interval, a conclusion already reached by the light scattering experiment. The increase in E_T with f_c thus provides a sensitive measure for micelle formation.

We have also measured the decay profiles, using the TCSPC method, of pyrene in polymer Ib as a function of f_c. Partially due to the fact that we did not deoxygenate the samples, the pyrene decay profiles were never single exponential. We analyzed the decay profiles by a two-term exponential fit. The mean pyrene

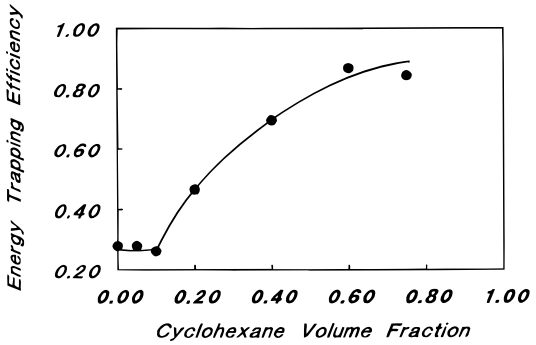

Figure 11. Increase in the energy trapping efficiency of polymer Ib at a fluorene labeling density of 2.4% as a function of f_c.

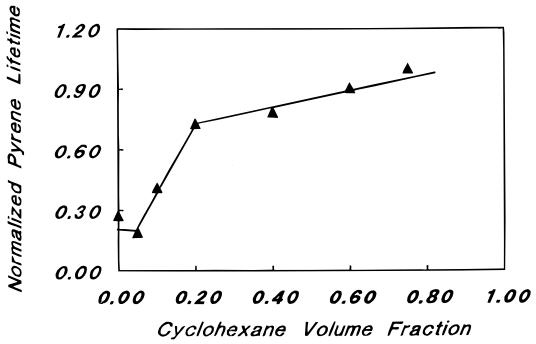

Figure 12. Normalized mean pyrene fluorescence lifetime $\langle\tau\rangle$ of polymer Ib as a function of cyclohexane content f_c. $\langle\tau\rangle = 75$ ns at $f_c = 0.75$.

fluorescence lifetimes were calculated using

$$\langle\tau\rangle = \sum_{i=1}^{2} a_i\tau_i \Big/ \sum_{i=1}^{2} a_i \qquad (14)$$

The change in the mean lifetime $\langle\tau\rangle$ of pyrene as a function of f_c is plotted in Figure 12. $\langle\tau\rangle$ increases rapidly between $f_c = 0.05$ and 0.20. This is attributed to the effect of micelle formation. As micelle forms, pyrene may become partially buried inside the micellar core. The viscosity inside a micellar core is high and the quenching of pyrene fluorescence by oxygen would be less efficient.

The increase in $\langle\tau\rangle$ slowed down after $f_c = 0.20$. One logical explanation is that $\langle\tau\rangle$ of pyrene increased very fast initially due to the incorporation of an increasing number of chains into micelles as the critical micelle concentration decreased with increasing f_c. At $f_c = 0.20$, most chains would have been incorporated. Further increase in $\langle\tau\rangle$ of pyrene after $f_c = 0.20$ derives from the tightening of the micellar core and thus the further increase in the core viscosity, which led to further reduction in the rate of pyrene fluorescence by oxygen. This also explains why E_T would increase continuously with f_c after $f_c = 0.20$ even though R_H and p are constant. The tightening of the micelle core with an increasing amount of poor solvent is in agreement with the spirit of Munch and Gast's prediction.[9]

IV. Conclusion

We have successfully synthesized PS-*b*-PHEMA and PS-*Py*-PHEMA for fluorescence studies. PS-*b*-PHEMA formed micelles in THF/cyclohexane mixtures. Of the two polymers studied, polymer II formed more stable micelles, and polymer Ia micelles were stable only at $f_c \leq 0.60$ or at f_c up to 0.75 if polymer concentration was lower than ~3 mg/mL. Polymer II formed micelles with an aggregation number of ~126 and a hydrodynamic radius of ~30 nm. These are larger than the corresponding values of 64 and 14 nm for polymer Ia micelles, in agreement with theoretical predictions. While the hydrodynamic radius of polymer II micelles was found to change slightly with the solvent composition, the aggregation numbers of micelles of both diblock copolymers were found to be invariant with the solvent composition.

Preliminary fluorescence experiments have concluded that energy transfer efficiency is very sensitive to micelle formation. Inside a micellar core, fluorene excimer formation was negligible even at the fluorene labeling density of 10%. Fluorene fluorescence quenching by pyrene has been found to be efficient, and energy transfer has been verified to be the dominant quenching mechanism. These features of donors and acceptors should facilitate the subsequent determination of the core radius of PHEMA by energy migration studies and the determination of chain exchange rate constant by mixing donor-labeled micelles and acceptor-labeled unimer. Our fluorescence results also suggest that the size of micelle cores shrinks as the solvent worsens for the core block.

Acknowledgment. The authors thank NSERC of Canada for financial support of this research,. G.L. wishes to thank his colleague, Prof. William G. Laidlaw, for his invaluable help in many ways. The use of dynamic light scattering facilities in Prof. J. Vancso's laboratory of the University of Toronto and Dr. G. Fytas' laboratory in the Institute of Electronic Structure & Laser is also gratefully acknowledged.

References and Notes

(1) Hunter, R. J. *Foundations of Colloid Science*; Clarendon Press: Oxford, 1986.
(2) Tuzar, Z.; Kratochvil, P. *Surf. Colloid. Sci.* **1992**, *15*, 1.
(3) Halperin, A.; Tirrell, M.; Lodge, T. P. *Adv. Polym. Sci.* **1992**, *100*, 31.
(4) Gast, A. P. In *Scientific Methods for the Study of Polymer Colloids and Their Applications*; Candau, F., Ottewill, R. H., Eds.; Kluwer Academic Publishers: Amsterdam, 1990.
(5) Daoud, M.; Cotton, J. P. *J. Phys. (Paris)* **1982**, *43*, 531.
(6) Leibler, L.; Orland, H.; Wheeler, J. C. *J. Chem. Phys.* **1983**, *79*, 3550.
(7) Halperin, A. *Macromolecules* **1987**, *20*, 2943.
(8) Grest, G. S.; Kremer, K.; Witten, T. A. *Macromolecules* **1987**, *20*, 1376.
(9) Munch, M. R.; Gast, A. P. *Macromolecules* **1988**, *21*, 1360.
(10) Balsara, N. P.; Tirrell, M.; Lodge, T. P. *Macromolecules* **1991**, *24*, 1975.
(11) Gao, Z.; Eisenberg, A. *Macromolecules* **1993**, *26*, 7353.
(12) Izzo, D.; Marques, C. M. *Macromolecules* **1993**, *26*, 7189.
(13) Watanabe, A.; Matsuda, M. *Macromolecules* **1986**, *19*, 2253.
(14) Major, M. D.; Torkelson, J. M.; Brearley, A. M. *Macromolecules* **1990**, *23*, 1700.
(15) Wilhelm, M.; Zhao, C.-L.; Wang, Y.; Xu, R.; Winnik, M. A.; Mura, J.-L.; Riess, G.; Croucher, M. D. *Macromolecules* **1991**, *24*, 1033.
(16) Astafieva, I.; Zhong, X. F.; Eisenberg, A. *Macromolecules* **1993**, *26*, 7339.
(17) Gao, Z.; Varshney, S. K.; Wong, S.; Eisenberg, A. *Macromolecules* **1994**, *27*, 7923.
(18) Kiserow, D.; Prochazka, K.; Ramireddy, C.; Tuzar, Z.; Munk, P.; Webber, S. E. *Macromolecules* **1992**, *25*, 461.
(19) Qin, A.; Tian, M.; Ramireddy, C.; Webber, S. E.; Munk, P.; Tuzar, Z. *Macromolecules* **1994**, *27*, 120.
(20) Alexandridis, P.; Holzwarth, J. F.; Hatton, T. A. *Macromolecules* **1994**, *27*, 2414.
(21) Halperin, A.; Alexander, S. *Macromolecules* **1989**, *22*, 2403.
(22) Ligoure, C.; Liebler, L. *J. Phys. (Paris)* **1990**, *51*, 1313.
(23) Johner, A.; Joanny, J.-F. *Macromolecules* **1990**, *23*, 5299.

(24) Procházka, K.; Bednár, B.; Mukhtar, E.; Svoboda, P.; Trnëná, J.; Almgren, M. *J. Phys. Chem.* **1991**, *95*, 4563.
(25) Bednár, B.; Edwards, K.; Almgren, M.; Tormod, S.; Tuzar, Z. *Makromol. Chem., Rapid Commun.* **1988**, *9*, 785.
(26) Wang, Y.; Kausch, C. M.; Chun, M.; Quirk, R. P.; Mattice, W. L. *Macromolecules* **1995**, *28*, 904.
(27) Chan, J.; Fox, S.; Kiserow, D.; Ramireddy, C.; Munk, P.; Webber, S. E. *Macromolecules* **1993**, *26*, 7016.
(28) (a) Ikemi, M.; Odagiri, N.; Tanaka, S.; Shinohara, I.; Chiba, A. *Macromolecules* **1981**, *14*, 34. (b) *Ibid.* **1982**, *15*, 281.
(29) Hruska, Z.; Piton, M.; Yekta, A.; Duhamel, J.; Winnik, M. A.; Riess, G.; Croucher, M. D. *Macromolecules* **1993**, *26*, 1825.
(30) Liu, G. *J. Phys. Chem.* **1995**, *99*, 5465.
(31) Liu, G. *Can. J. Chem.*, in press.
(32) Hirao, A.; Kato, H.; Yamaguchi, K.; Nakahama, S. *Macromolecules* **1986**, *19*, 1295.
(33) Quirk, R. P.; Schock, L. E. *Macromolecules* **1991**, *24*, 1237.
(34) Morton, M. *Anionic Polymerization: Principles and Practice*; Academic Press: New York, 1983.
(35) Gerrard, W.; Thrush, A. M. *J. Chem. Soc.* **1952**, 741.
(36) Huglin, M. B. *Light Scattering from Polymer Solutions*; Academic Press: London, 1971.
(37) Weast, R. C. *CRC Handbook of Chemistry and Physics*, 70th ed.; CRC Press: Boca Raton, FL, 1990.
(38) Berlman, I. B. *Handbook of Fluorescence Spectra of Aromatic Molecules*; Academic Press: New York, 1971.
(39) Brandrup, J.; Immergut, E. H. *Polymer Handbook*, 3rd ed.; John Wiley & Sons: New York, 1989.
(40) Horrocks, D. L.; Brown, W. G. *Chem. Phys. Lett.* **1970**, *5*, 117.
(41) (a) Liu, G.; Guillet, J. E. *Macromolecules* **1990**, *23*, 1388. (b) Liu, G.; Guillet, J. E.; Al-Takrity, E. T. B.; Jenkins, A. D.; Walton, D. R. M. *Ibid.* **1990**, *23*, 1393.

MA9503930